Bimodality and Long-Term Trends of the Extreme Values of Air Temperature

Ján Pekár[1)], Pavla Pekárová[2*)], Pavol Miklánek[3)]

[1)] Comenius University in Bratislava, Faculty of Mathematics, Physics, and Informatics, Mlynská dolina, 842 48 Bratislava, Slovakia; https://orcid.org/0000-0003-2263-287X
[2)] Slovak Academy of Sciences, Institute of Hydrology, Dúbravska cesta 9, 841 04 Bratislava, Slovakia; email: pekarova@uh.savba.sk; https://orcid.org/0000-0002-1180-2215
[3)] Slovak Academy of Sciences, Institute of Hydrology, Dúbravska cesta 9, 841 04 Bratislava, Slovakia; https://orcid.org/0000-0001-5075-6445

http://doi.org/10.29227/IM-2024-01-24

Submission date: *15.4.2023* | Review date: *7.5.2023*

Abstract

Histograms of air temperature with a bimodal shape are commonly observed in many regions of the world. In this study, we investigate the causes of bimodality in the histograms of daily temperature series (minimum, average, and maximum) for selected climatological stations in Slovakia. Our findings suggest that in the Central European region, the bimodal shape of air temperature histograms is mainly due to the latent heat of freezing, as the surface of snow and ice and the air are thermally coupled. The asymmetry in the air temperature histograms is due to the lower mass heat capacity of ice compared to water and air. The energy-intensive latent heat of conversion of ice to water (and vice versa) results in the more frequent occurrence of ground-layer air temperatures around the freezing point, leading to the formation of the observed local maximum. This has far-reaching implications, such as the calculation of the annual mean air temperature at climatological stations. When calculating the average air temperature, negative temperatures should be given less weight than positive temperatures. Temperatures around 0-6°C should be given higher weight. This may also explain why Arctic regions are experiencing more significant warming than equatorial regions. In the second part of this paper, we analyze the long-term trends of selected temperature indices for the climatological station at Hurbanovo (Slovakia) from 1871 to 2020. Our results indicate statistically significant changes in all temperature indices, with indices related to cold temperatures increasing more significantly than those associated with high temperatures. Finally, study examines theoretical probability distributions to estimate T-year temperatures for temperature indices at the Hurbanovo climate station in Slovakia. The analysis includes three time periods (1901–1960, 1961–2020, and 1991–2020) and reveals significant changes in temperature indices at the Hurbanovo station. The 100-year temperature of TN,min was –35.75°C in 1901–1960, –28.69°C in 1961–2020, and –26.52°C in 1991–2020. The 100-year temperature of TX,max was 39.4°C in 1901–1960 and 39.63°C in 1961–2020. TN,min showed the most significant changes, with the 100-year temperature increasing by up to 7.06°C in 1961–2020 and up to 9.23°C in 1991–2020.

Keywords: bimodality, long-term trends, extreme values, air temperature

Introduction

When dealing with issues related to climate change, such as the increase in extreme air and water temperatures, it is often necessary to create a histogram and determine the distribution function of a series of measured minimum, maximum, or average daily temperature values. Many natural processes follow unimodal distribution functions with symmetric shapes, particularly for time series of mean annual air temperature or seasonal air temperature. The distribution of mean daily surface air temperature measured at climatological stations located in continental warm regions near the equator typically exhibits normal (Gaussian) unimodality, as seen at stations in Brasilia (Figure 1) [1, 2]. In coastal areas, air temperature is influenced by seawater temperature, resulting in a bimodal histogram of mean daily temperatures (Alicante, Spain). In inland cold temperate regions, one peak of the histogram is typically around 0°C–6°C (e. g. Kingston, Canada).

There is a continuous exchange of moisture between the active surface, soil, and the atmosphere. When analysing air temperature, it is important to consider that water exists in three states.

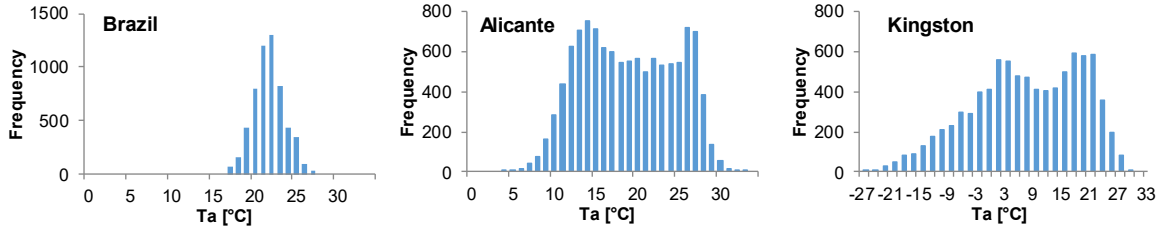

Fig. 1. Examples of the mean daily air temperature histograms from different continents selected from Gasparrini et al. (2015)

The water content of the atmosphere affects several processes in the atmosphere, including air temperature. This complicates the ability to derive a theoretical distribution function of daily air temperature series. As a result, estimating the distribution of daily (minimum, average, maximum) air temperatures in the future, based on historical observations, will not be a linear process due to the influence of changing water content in the atmosphere as it warms up.

Understanding how daily air temperature characteristics will evolve in the future is crucial for every country, as air temperature impacts every aspect of society. Reliable estimates of future extreme air temperatures are vital for public health, agriculture, hydrology, engineering, the economy, and more [2-5].

In the first part of the paper, the long-term trends of selected average, minimum, and maximum air temperature indices at the Hurbanovo and Liptovský Hrádok climatological stations in Slovakia from 1871 to 2020 are examined. In the second part, the bimodality of air temperature and water temperature histograms is investigated, with several examples from the High Tatra Mountains region provided to illustrate why mean daily surface air temperature exhibits asymmetric histograms with a bimodal shape. Finally, the paper estimates the design values of various air temperature indices at the Hurbanovo station.

Materials

We constructed the empirical histogram of air temperature using the minimum T_N, mean T_d, and maximum T_X daily air temperature series observed over the period 1961–2010 at five climatological stations located in the region of the High Tatras (Slovakia) (Table 1). The Institute of Meteorology and Water Management in Poland collects data from the observatory station at Kasprowy Wierch. These stations and the region of the High Tatras were selected because they are relatively unaffected by anthropogenic activities.

To analyze the long-term trend of air temperature, we used the mean daily air temperature series observed over a period of 150 years from the Hurbanovo observatory, during 1871–2020. The Hurbanovo station, previously known as Ógyalla – Stará Ďala, is an ideal station for studying the relatively arid region of the Danubian lowland region [6- 10]. It is considered one of the best meteorological stations in Central Europe, providing long, high-quality, and homogeneous observations. The meteorological observatory is located in the large garden on the northern edge of the small city of Hurbanovo. Regular measurements of air temperature [°C] and precipitation [mm] started in 1876 at this station, with the period 1871–1875 completed using data from the Komárno station (located 20 km from Hurbanovo). The Slovak Hydrometeorological Institute (SHMI) maintains the data collected from this station.

The air temperature observations were carried on a climatic schedule at 7 a.m. (T_7), 2 p.m. (T_{14}), and 9 p.m. (T_{21}) in the middle local time in Slovakia. The daily mean of air temperature (T_d) was recalculated according to the formula: $T_d = (T_7 + T_{14} + 2T_{21})/4$. The minimum thermometer was used to measure the instantaneous minimum air temperature (T_N) and the maximum thermometer was used to measure the instantaneous maximum temperature (T_X) each day. In table 1 there are presented the basic temperature data on the stations under study.

We assembled the following series of temperature indices in °C for each station. The measured series of daily values are boldly highlighted:

T_d series of mean daily air temperature (365/366 data per year);
$T_{d,avg}$ series of mean annual air temperature (1 datum per year);
$T_{d,max}$ series of maximum mean daily air temperature (1 datum per year);
$T_{d,min}$ series of minimum mean daily air temperature (1 datum per year);
T_X series of instantaneous maximum daily air temperature (365/366 data per year);
$T_{X,max}$ series of maxima of the instantaneous maximum daily air temperature (1 datum per year);
T_N series of instantaneous minimum daily air temperature (365/366 data per year;)
$T_{N,min}$ series of minima of the instantaneous minimum daily air temperature (1 datum per year).

In addition to the air temperature data, we analysed time series of daily water temperature measured at 7 a.m. in the mountainous Belá River (at water gauges: Podbanské and Liptovský Hrádok) and in the Váh River (at the water gauge Liptovský Mikuláš), with the first temperature measurements taken in 1960 (table 2). The water temperature data were acquired from the database of the SHMI. It should be noted here that experimental measurements of air and water temperature were also carried out with shorter time intervals (minute, hour) by the Institute of Hydrology of the Slovak Academy of Sciences [11].

Tab. 1. Basic characteristics of the selected air temperatures in climatic stations. The elevation of station – H; long-term mean daily air temperature in °C at the station - $T_{d,avg,a}$; minimum of mean daily temperature - $T_{d,min,a}$; maximum of mean daily air temperature - $T_{d,max,a}$. Period 1961–2010

Station	H [m a.s.l.]	Td,avg,a [°C]	Td,min,a [°C]	Td,max,a [°C]	Geogr. altitude			Geogr. longitude		
Hurbanovo	115	10.41	-20.3	31.3	47	52	23	18	11	39
Liptovský Mikuláš	569	7.01	-23.5	26.7	49	5	52	19	35	32
Liptovský Hrádok	640	6.59	-23.5	25.9	49	2	21	19	43	31
Podbanské	972	5.04	-22.1	24.0	49	8	24	19	54	38
Štrbské Pleso	1322	3.67	-21.8	23.1	49	7	10	20	3	48
Kasprowy Wierch	1998	-0.54	-27.0	17.8	49	13	57	19	58	55
Lomnický štít	2635	-3.56	-30.9	14.1	49	11	43	20	12	54

Tab. 2. Basic characteristics of the selected water temperature series. The water gauge level zero – H; area of the basin – A, long-term average of the water temperature measured at 7 a.m. in °C - $T_{7,avg,a}$; minimum water temperature - $T_{7,min,a}$; maximum of water temperature - $T_{7,max,a}$. 1961–2010

River - station	H [m a.s.l.]	A [km2]	T7,avg,a [°C]	T7,min,a [°C]	T7,max,a [°C]
Váh - Liptovský Mikuláš	566	1107.2	6.15	0.0	18.7
Belá -Liptovský Hrádok	630	244.26	5.10	0.0	17.8
Belá - Podbanské	922	93.49	4.30	0.0	9.5

Methods

In this study, our aim was to detect the trend point changes in time series. In trend analysis of time series, the null hypothesis H_0 is usually tested against the alternative hypothesis H_1, where H_0 suggests that there is no trend and H_1 suggests that there is a trend. Parametric and non-parametric tests can be used for this purpose. In our study, we used the non-parametric Mann-Kendall test, which is widely used for detecting significant trends in time series. Non-parametric tests are more appropriate for detecting trends in hydro-meteorological time series, which are often irregular and have many extremes. Our study involves two types of statistical analyses: 1) testing for the presence of a monotonic increasing or decreasing trend, and 2) estimating the slope of a linear trend using the non-parametric Sen's method, which assumes that the variance of the residuals is constant over time. Generally, the most common assumptions in change point hypothesis testing are normality (population is distributed normally) and statistical independence (randomness) of observations. Correct application of the change point tests is facilitated by the fact that the tests are divided into three groups: tests assuming both normality and independence, tests assuming normality, and tests assuming independence.

Histograms and distribution functions

In meteorology and climatology, the estimation of design values of occurrence or exceedance of the air temperature with a certain probability is done using the theoretical functions of probability density distribution (distribution function). Analysing the 60-year series of observations we can reliably estimate the extreme values with the mean probability of exceedance up to once per 100 years. These values are recently been frequently applied in several branches [12, 13].

The selection of the theoretical distribution function is based on empirical histograms. Histograms belong to elementary statistical methods of graphical processing of the time series of extensive data sets. They are used to display the frequency of occurrence of certain values sorted into classes and they help to develop the theoretical distribution curves of occurrence or exceedance.

The histograms can have different shapes like unimodal (single-peak) or multimodal (multi-peak). The series of mean daily air temperatures in the Carpathian region in Central Europe have the bimodal (two-peak) asymmetric histogram. It is not allowed to describe the distribution curve of the bimodal distribution by such one with a unique peak computed from the mean value and standard deviation of the bimodal distribution. In the case of bimodal histograms, it is necessary to split the distribution into subsets taking into account their character.

Results

Long-term trends and variability of air and water temperature in Slovakia

The basic assumption to estimate the distribution functions of the temperature series is the homogeneity and stationarity of the measured time series [14]. In this study, we analysed the long-term trends and multiannual fluctuations of air temperature using the series of mean annual air temperature at Hurbanovo and Liptovský Hrádok stations, which are the longest measured homogenous series in Slovakia [6, 7, 8, 9, 15, 16].

Long-term trends of the other air temperature indices at Hurbanovo are shown in Figure 2. The following five series of air temperature indices were processed:

$T_{N,min}$ series of minima of the instantaneous minimum daily air temperature (1 datum per year)
$T_{d,min}$ series of minimum mean daily air temperature (1 datum per year)
$T_{d,avg}$ series of mean annual air temperature (1 datum per year)
$T_{d,max}$ series of maximum mean daily air temperature (1 datum per year)

$T_{X,max}$ series of maxima of the instantaneous maximum daily air temperature (1 datum per year)

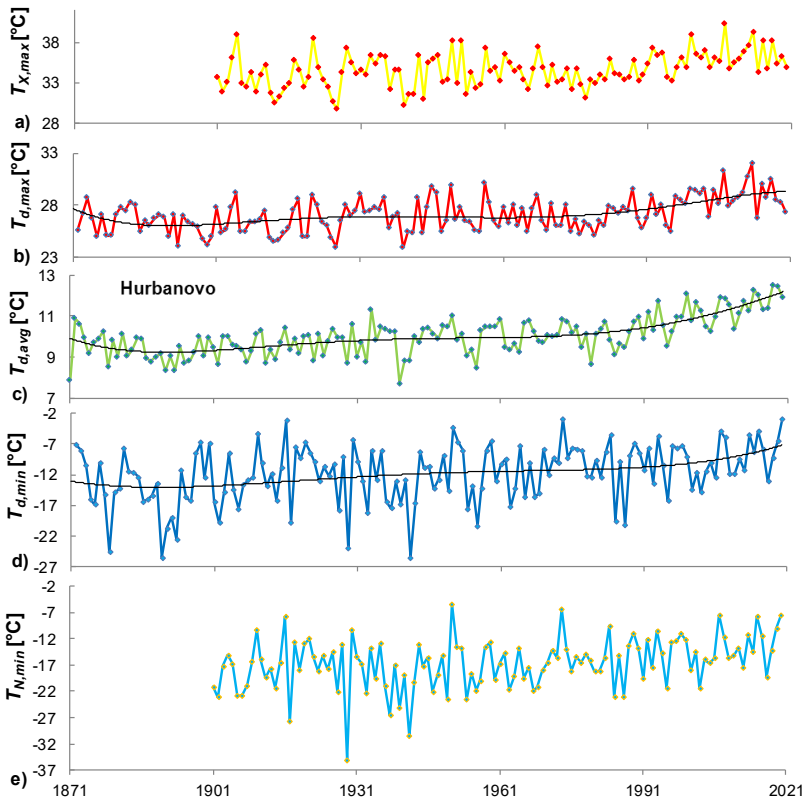

Fig. 2. The course of the selected five air temperature characteristics at station Hurbanovo in °C, for the period 1871/1901–2020

First of all, we identified the breakpoints of the long-term linear trend at Hurbanovo and Liptovský Hrádok stations in the average annual temperature time series. There were two points identified: in 1900 and 1990 [17]. In Hurbanovo, the identified trend was declining (slope = –0.0246) in the first period 1871–1900; the air temperature grew slightly (slope = 0.0079) in the second period, and there was a sharp rise in air temperature (slope = 0.0491) in the third period, after 1990.

To identify multiannual fluctuations of the annual air temperature time series, we created a series of residuals for both stations by removing the linear trend. We used autocorrelation and spectral analysis for identification. Figure 3 shows the autocorrelogram and periodogram of annual air temperature time series residuals in Hurbanovo. We identified a significant 7 to 8-year cycle of alternating warmer and colder periods.

The air temperature trends in other Slovak stations with shorter observations show a similar increasing pattern. These results are in line with the trend of increasing air temperature observed in Europe and other regions. Based on the trend analysis, it can be concluded that temperature series are not stationary. One way to circumvent non-stationarity of data is to divide a long time period into shorter periods.

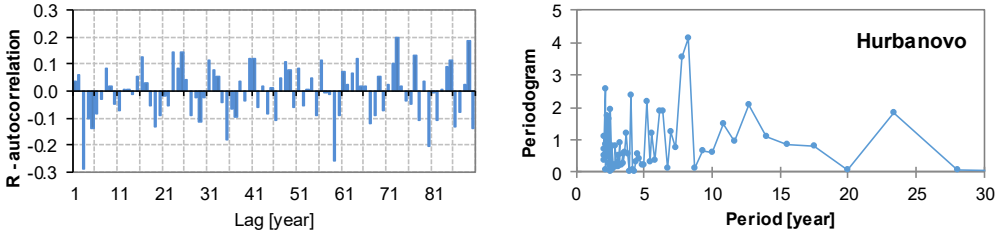

Fig. 3. Autocorrelogram (left) and periodogram (right) of the yearly temperature residuals, Hurbanovo station, period 1871–2020

Long-term trends and variability of air and water temperature in Slovakia

Histograms of the 50-year series of mean daily air temperature for six selected stations with different altitudes are presented in Figure 4a. Five of the histograms are based on data from the High Tatras region, while one is from the lowland station of Hurbanovo. A comparison of histograms of mean daily air temperature observed at the climatological station in Liptovský Mikuláš and water temperature measured in the Váh River at Liptovský Mikuláš is illustrated in Figure 4b. Similarly, histograms of air temperature from the climatological station at Liptovský Hrádok and water temperature measurements in the Belá River (water gauge Liptovský

Hrádok) taken during the period 1961–2010 are also shown in Fig. 4b. The histograms show a bimodal shape for the climatological stations located at lower elevations with mean annual air temperature over +1°C. The first peak is located in the class interval around 0 to +2°C

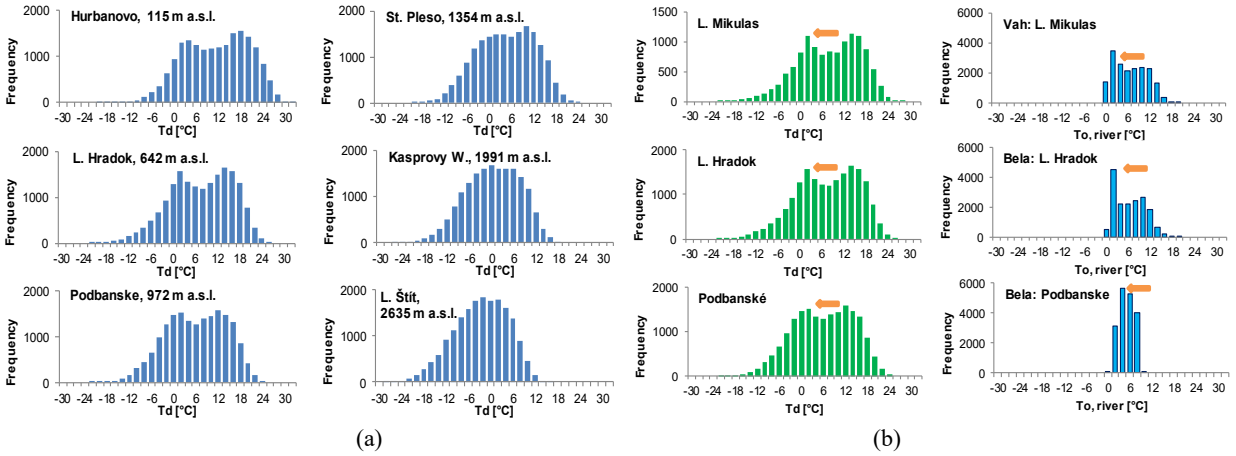

Fig. 4. a) Histograms of the mean daily air temperature series (Td) in selected climatic stations, period 1961–2010. b) Histograms of the mean daily air temperature (left charts) at Liptovský Mikuláš, Liptovský Hrádok and Podbanské, and water temperature measured at 7 a.m. (right charts) of the Váh River at Liptovský Mikuláš and Belá River at Liptovský Hrádok and Podbanské during 50-years period 1960–2010

The histograms of water temperature have a smaller dispersion and are lower bounded - the minimum observed water temperature in the rivers is 0°C. It is evident that temperatures around +2°C are the most frequently observed. We have previously shown in our studies [18] that the mean annual water temperature is related to the mean annual air temperature in the vicinity of the water gauging station.

The reason for a higher frequency of mean daily air temperatures between 0 and +2°C can be attributed to latent heat. When water freezes, latent heat is liberated. In the winter season, the surface of snow and ice and the adjacent air above are thermally coupled [19]. On the molecular level, when heat is taken from liquid water, the motion of water molecules slows down until ice/snow develops. The surrounding air receives the energy the water molecules once had to rotate, a process accompanied by increasing air temperature. This energy is called the latent heat of freezing. This latent heat of freezing temporarily prevents the air temperature from continuing to cool below 0°C. Our data demonstrate that the temperatures between 0 to +2°C occur with a higher frequency (Figure 4a), except for the stations at Kasprowy Wierch, Lomnický Štít – where the mean annual air temperature is below 0°C – the two peaks merge into a single peak forming a unimodal histogram.

The mass heat capacity of ice is half that of water and a quarter that of air. Water has a specific heat capacity of c = 4.180 $kJ.kg^{-1}.K^{-1}$, ice 2.090 $kJ.kg^{-1}.K^{-1}$, and dry air at sea level 1.0035 $kJ.kg^{-1}.K^{-1}$. Therefore - given the same amount of heat - the temperature of dry air at negative values increases faster than the temperature of moist air at positive values of air temperature (cause of asymmetry in the histograms of air temperature). Furthermore, note that the latent heat of fusion of the ice melting is 334.0 $kJ.kg^{-1}$, therefore, because of the change of the ice to water and vice versa in the vicinity of the station, air temperatures around zero occur more frequently.

For clarification, Fig. 5 shows the time history of the heating temperature of ice with a mass of 1 kg from an initial temperature of -20°C (with a heating power of 1 kW). When the ice temperature reaches 0°C, the temperature rise stops and the ice starts to melt. The temperature remains constant until all the ice has melted. As mentioned, the mass latent heat of the fusion of ice is 334.0 $kJ.kg^{-1}.K^{-1}$, so for the chosen energy consumption and ice mass, 1 kg of ice will take 334 s to melt. After that, the temperature will start to increase again, with the steepness of the curve at temperatures from 0°C to 100°C being half that of the curve at temperatures below 0°C. This is because the mass heat capacity of water is approximately twice that of ice. This phenomenon gives rise to a second peak in the histograms.

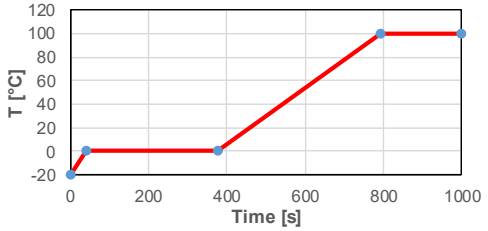

Fig. 5. The course of temperature during heating of ice with a mass of 1 kg over time from an initial temperature of -20°C to 100°C (for 1 kW heating)

The peak in the histogram is shifted towards higher values of air temperature due to atmospheric warming. Figure 6 presents histograms of minimum daily air temperature measured at Hurbanovo over two 30-year periods: 1901–1930 and 1991–2020. As illustrated, the bimodal shape of the histogram has been preserved in both periods, but it has shifted toward higher temperatures,

especially in the section of high temperatures. Interestingly, there is no shift in the first peak of the histogram at minimum temperatures between –2 and +2°C, which confirms our hypothesis that this peak is related to the freezing of water and melting of snow/ice in the vicinity of the station. Moreover, the histograms are asymmetric.

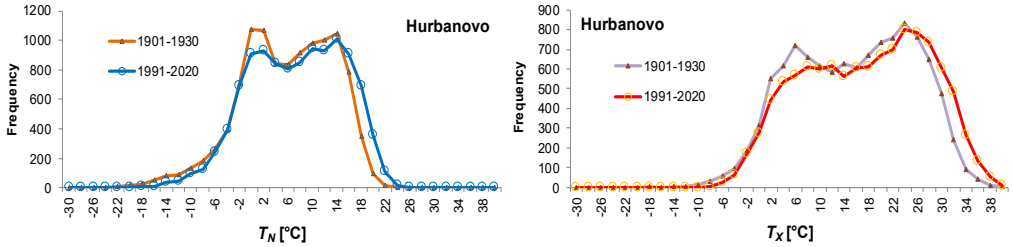

Fig. 6. Comparison of minimum (left) and maximum daily air temperature histograms for two 30-year periods 1901–1930 and 1990–2020, Hurbanovo station

Design values of various air temperature indices at the Hurbanovo station

Choosing a proper theoretical distribution for the mean, maximum, and minimum daily air temperature with a multimodal distribution is a complex problem [20, 21]). There are several approaches to estimating the *T*-year values of the selected temperature indices:

1. Splitting a bimodal histogram into two unimodal histograms. Figure 7 presents the histogram distribution of the instantaneous daily minima (T_N); mean daily (T_d) and instantaneous daily maxima (T_X) of the air temperature series at Hurbanovo into two distributions, the distribution function for the higher temperatures is symmetric.
2. To avoid this problem, other solution is to use theoretical distribution curves for each day or month of the year. These histograms have only one peak, and in some cases, it is possible to estimate *T*-year design values by applying a normal or log-normal distribution function. As shown in the figures, the histograms are asymmetric, with temperatures around 0°C occurring more frequently during the winter months of December to February. Histograms in April and October have very similar shapes.
3. The third approach to estimating the *T*-year design values of extreme air temperature is to select time series consisting of one value per year, such as the maximum or minimum annual air temperature series

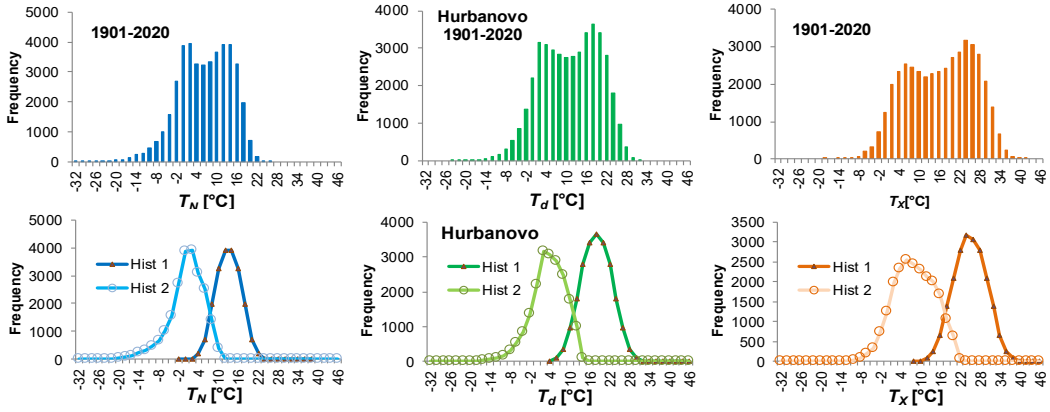

Fig. 7. Bimodal histograms of the instantaneous daily minima (T_N); mean daily (T_d) and instantaneous daily maxima (T_X) of the air temperature series at the Hurbanovo, Slovakia station, period 1901–2020 (upper). Splitting of bimodal histograms into two unimodal histograms (lower)

Finally, we have calculated the *T*-year values of extreme air temperature observed at the Hurbanovo station for the whole period 1901–2020; for two 60-years sub-periods 1901–1960 and 1961–2020, and for short last 30-years period 1991–2020. 3. The third approach and the following data sets (all of them with 1 datum per year) were used:

$T_{X,max}$ - series of maxima of the instantaneous maximum daily air temperature,
$T_{d,max}$ -series of maximum mean daily air temperature,
$T_{d,avg}$ - series of mean annual air temperature,
$T_{d,min}$ series of minimum mean daily air temperature, and
$T_{N,min}$ - series of minima of the instantaneous minimum daily air temperature.

The aim is to assess the change in *T*-year extremes of air temperature with long return periods. The basic statistical characteristics of the temperature indices calculated for two periods for the Hurbanovo station are presented in table 3. The minimum *T*-year air temperature increased significantly more than the *T*-year maximum air temperature during the 60-year period at the station Hurbanovo. In Figure 8, the two sample comparison is visualized.

The statistical tests have shown, that it is possible to use the log-normal probability distribution function to estimate the *T*-year values of the temperature indices. Table 4 lists the estimated *10*-, *100*- and *200*- year air temperatures for the three sub-periods. The estimated *200*-year minimum air temperature increased by more than 7°C in period 1961–2020 (from –38.67°C to –30.82°C), while by more than 10°C in period 1991–2020 (from –38.67°C to –28.48°C). The maximum *200*-year air temperature increased

only by 0.11°C (from 40.03°C to 40.14°C), resp. by 0.58°C in period 1991–2020. In the case of estimation of the *T*-year values from the $T_{N,min}$ series, time series $T_{N,min}$ was multiplied by –1. Then were calculate *T*-year values for the upper tail of the $-T_{X,max}$ series. Finally, calculated *T*-year values were multiplied by –1, and it was *T*-year values of the lower tail $T_{N,min}$.

Tab. 3. Basic statistical characteristics of selected air temperature series (in °C) from station Hurbanovo in two periods P: 1. 1901–1960, and 2. 1960–2020

Statistic / Period	*TN,min 1*	*TN,min 2*	*Td,min 1*	*Td,min 2*	*Td 1*	*Td 2*	*Td,max 1*	*Td,max 2*	*TX,max 1*	*TX,max 2*
Minimum	-35.00	-23.0	-25.50	-20.3	7.71	8.67	23.9	25.1	29.8	31.2
1st Quartile	-21.18	-18.0	-15.23	-12.2	9.28	10.0	25.5	26.4	32.5	33.7
Median	-17.45	-15.4	-12.80	-9.6	9.92	10.6	26.5	27.8	34.1	34.9
3rd Quartile	-14.40	-12.6	-8.83	-7.8	10.2	11.2	27.8	28.8	35.5	36.2
Maximum	-5.40	-6.3	-3.20	-2.9	11.3	12.5	30.2	32.0	39.0	40.3
Mean	-18.00	-15.3	-12.52	-10.1	9.75	10.6	26.7	27.7	34.0	35.1
Diff. of means	2.7		2.33		0.89		0.95		1.1	
Variance (n-1)	27.8	15.6	21.6	13.8	0.50	0.81	2.38	2.53	4.69	3.38
Stand. Dev. (n-1)	5.27	3.9	4.6	3.7	0.71	0.90	1.54	1.59	2.17	1.84
Stnd. skewness	-1.70	0.3	-1.4	-1.7	-1.4	0.53	0.95	1.31	0.87	1.52
Stnd. kurtosis	1.94	-.41	0.28	0.51	-.07	-0.9	-1.04	-0.40	-0.71	0.39

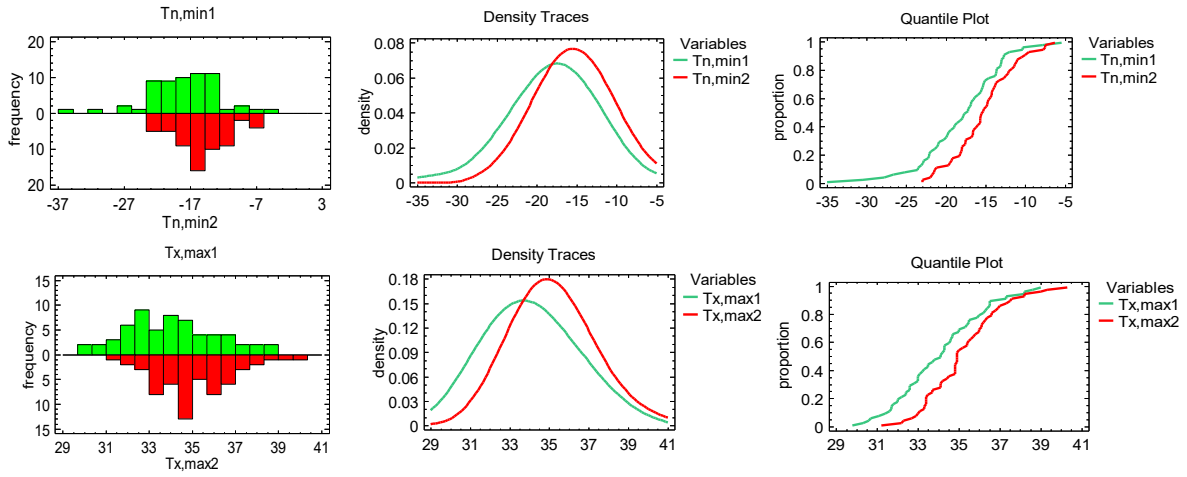

Fig. 8. Graphical plots of differences between two series $T_{N,min}$ and $T_{X,max}$ for two 60-years periods 1901–1960 and 1961–2020. From left - histograms; distribution densities; quantile plots. The values on the horizontal axis correspond to air temperature in °C

Tab. 4. T-year air temperature in station Hurbanovo in three sub-periods P: 1. 1901–1960; 2. 1961–2020; 3. 1991–2020, and whole period 1901–2020. Difference Diff between T-year temperatures estimated for the first and second, resp. third periods

	P	*TN,min*	*Diff*	*Td,min*	*Diff*	*Td,max*	*Diff*	*TX,max*	*Diff*
10-year temp. °C	1.	-25.74		-19.56		28.78		36.88	
	2.	-21.27	4.47	-15.78	3.78	29.79	1.01	37.54	0.66
	3.	-19.66	6.08	-14.76	4.80	30.56	1.78	38.33	1.45
	4.	-23.67		-17.82		29.37		37.32	
100-year temp. °C	1.	-35.75		-29.90		30.56		39.40	
	2.	-28.69	7.06	-23.90	6.00	31.62	1.06	39.63	0.23
	3.	-26.52	9.23	-22.29	7.61	32.27	1.71	40.16	0.76
	4.	-32.70		-27.43		31.26		39.73	
200-year temp. °C	1.	-38.67		-33.09		31.00		40.03	
	2.	-30.82	7.85	-26.39	6.70	32.07	1.07	40.14	0.11
	3.	-28.48	10.19	-24.69	8.49	32.69	1.69	40.61	0.58
	4.	-35.33		-30.4		31.72		40.32	

Conclusions

The changing variability of extreme air temperatures over the last three decades has been the focus of climate scientists, hydrologists, farmers, and society as a whole, as it can have a significant impact on the global hydrological cycle and energy balance of the Earth.

An example of long-term changes in air temperature was presented for the Hurbanovo station covering the period 1871–2020. The results showed statistically significant changes in all temperature indices, with the indices related to cold negative temperatures in Slovakia increasing more significantly by about 3°C per 60 years. Conversely, the indices associated with high temperatures increased by 1°C per 60 years. Although the period 1950–1980 witnessed a few downward trends, significant increasing trends of all thermal indices were detected after the year 1985. In general, the total warming can be attributed mainly to the warming within the

period 1986–2020. These results are consistent with the findings of other authors from the region of Europe, as well as other regions of the world, e.g. [22].

The core of the article is formed by its second part. In this section, we clarify that the bimodal shape of the histograms of measured daily and extreme air temperature in the Central European region is due to the latent heat of freezing, which causes thermal coupling between the surface of snow/ice and the air. We propose that the asymmetry in the air temperature histograms is caused by the lower mass heat capacity of ice compared to water and air. The bimodality of the air temperature histogram is a result of the energy-intensive latent heat required for the conversion of ice to water (and vice versa), which consumes or releases heat (latent heat of melting and freezing). This results in more frequent ground-layer air temperatures around the freezing point and the formation of the observed local maximum.

Explaining this has far-reaching implications, for example, for the calculation of the annual mean air temperature at stations. When calculating the arithmetic air temperature average, the negative temperature should be weighted less than the positive. Temperatures around 0-6 ° C should be taken with higher weight. It is also a possible explanation for why the Arctic regions of the Earth are warming more significantly than the equatorial regions. This is also the reason why long-term average annual water temperatures are lower than average annual air temperatures (compare values in Tables 1 and 2).

Finally, we concentrated on the construction of theoretical probability distributions for the individual temperature indices to estimate *T*-year temperatures. In this study, we present the results from climate station in Hurbanovo. The analysis of distribution functions for three periods (1901–1960; 1961–2020; and 1991–2020) of various temperature indices indicates the significant changes at the Hurbanovo station. In the period 1901–1960, the *100*-year temperature of the series $T_{N,min}$ was –35.75°C, –28.69°C in the period 1961–2020 and –26.52°C in the 1991–2020. The *100*-year temperature of the series $T_{X,max}$ was 39.4°C in 1901–1960 and 39.63°C in the period 1961–2020. The most significant changes in the design values of temperatures occurred in the case of an index $T_{N,min}$, where the *100*-year temperature increased by up to 7.06°C resp. 9.23°C

Acknowledgments

This research is supported by the project APVV-20-0374 “Regional detection, attribution and projection of impacts of climate variability and climate change on runoff regimes in Slovakia”, and project WATSIM “Water temperature simulation during summer low flow conditions in the Danube basin”.

References

1. A. Gasparrini, Y. Guor, M. Hashizume, E. Lavigne; A. Zanobetti, J. Schwartz, A. Tobias, S. Tong, J. Rocklöv, B. Forsberg, M. Leone, M. De Sario, M. Bell, I. L. Guo, C. Wu, H. Kan, S. M. Yi, M. de Sousa, Z. S. Coelho, P. Hilario, N. Saldiva, Y. Honda, H. Kim and B. Armstrong, "Mortality risk attributable to high and low ambient temperature: a multicountry observational study", Lancet 386, is. 9991, 369–375 (2015). https://doi.org/10.1016/S0140-6736(14)62114-0
2. H. Y. Cho and S. T. Jeong, "Estimation and Comparative Analysis on the Distribution Functions of Air and Water Temperatures in Korean Coastal Seas", Journal of Korean Society of Coastal and Ocean Engineers 28, 3, 171–176 (2016). https://doi.org/10.9765/KSCOE.2016.28.3.171
3. C. I. Garfinkel and N. Harnik, "The non-Gaussianity and spatial asymmetry of temperature extremes relative to the storm track: The role of horizontal advection", J. Clim. 30, 2, 445–464 (2017). https://doi.org/10.1175/JCLI-D-15-0806.1
4. M. Matiu, D. P. Ankerst and A. Menzel, "Asymmetric trends in seasonal temperature variability in instrumental records from ten stations in Switzerland, Germany and the UK from 1864 to 2012", Int. J. Climatol. 36, 13–27 (2015). https://doi.org/10.1002/joc.4326
5. C. Shi, Z. H. Jiang, L. H. Zhu, X. Zhang, Y. Y. Yao and L. Lie, "Risks of temperature extremes over China under 1.5°C and 2°C global warming", Adv. Clim. Change Res. 11, 3, 172–184 (2020). https://doi.org/10.1016/j.accre.2020.09.006
6. S. Petrovič, Climate Conditions of Hurbanovo (Slovakia) (Hydrometeorological Institute, Prague, Czech Republic, 1960, in Slovak), pp. 138–161.
7. M. Konček, Climate of the Tatra Mountains (VEDA, Bratislava, Slovakia, 1974, in Slovak), 885 p.
8. M. Lapin, "Detection of changes in the regime of selected climatological elements at Hurbanovo", Contributions to Geophysics and Geodesy 34, 2, 169–193 (2004).
9. P. Faško, M. Lapin and J. Pecho, "20-year extraordinary climatic period in Slovakia", Meteorologický časopis 11, 99–105 (2008). https://www.shmu.sk/File/ExtraFiles/KMIS/pub_cinnost/Lapin_et_al_2008.pdf
10. D.Halmová, P. Pekárová, J. Olbřímek, P. Miklánek and J. Pekár, "Precipitation regime and temporal changes in the Central Danubian lowland region", Advances in Meteorology Article ID 715830, 12 pages (2015). https://doi.org/10.1155/2015/715830
11. P. Pekárová, P. Miklánek, D. Halmová, M. Onderka and J. Pekár, "Long-term trend and multi-annual variability of water temperature in the pristine Bela River basin (Slovakia)", J. Hydrol. 400, 3-4, 333–340 (2011). https://doi.org/10.1016/j.jhydrol.2011.01.048
12. J. Kyselý, "Mortality and displaced mortality during heat waves in the Czech Republic", Int J Biometeorol. 91–97 (2004). https://doi.org/10.1007/s00484-004-0218-2
13. L. V. Alexander, X. Zhang, T. C. Peterson, J. Caesar, B. Gleason, A. M. G. Klein Tank, M. Haylock, D. Collins, B. Trewin, F. Rahimzadeh, A. Tagipour, K. Rupa Kumar, J. Revadekar, G. Griffiths, L. Vincent, D. B. Stephenson, J. Burn, E. Aguilar, M. Brunet, M. Taylor, M. New, P. Zhai, M. Rusticucci and J. L. Vazquez-Aguirre, "Global observed changes in daily climate extremes of temperature and precipitation", J. Geophys. Res. 111, D05109 (2006). https://doi.org/10.1029/2005JD006290
14. P. Liang, Z. W. Yan and Z. Li, "Climatic warming in Shanghai during 1873–2019 based on homogenised temperature records", Adv. Clim. Change Res. 1, 4, 496–506 (2022). https://doi.org/10.1016/j.accre.2022.05.006
15. J. Spinoni, S. Szalai, T. Szentimrey, M. Lakatos, Z. Bihari, A. Nagy, A. Németh, T. Kovács, D. Mihic, M. Dacic, P. Petrovic, A. Kržič, J. Hiebl, I. Auer, J. Milkovic, P. Štepánek, P. Zahradnícek, P. Kilar, D. Limanowka, R. Pyrc, S. Cheval, M. V. Birsan, A. Dumitrescu, G. Deak, M. Matei, I. Antolovic, P. Nejedlík, P. Štastný, P. Kajaba, O. Bochnícek, D. Galo, K. Mikulová, Y. Nabyvanets, O. Skrynyk, S. Krakovska, N. Gnatiuk, R. Tolasz, T. Antofie and J. Vogt, "Climate of the Carpathian Region in the period 1961–2010: climatologies and trends of 10 variables", Int J Climatol. 35, 1322–1341 (2014). https://doi.org/10.1002/joc.4059.
16. L. Labudová, P.Faško and G. Ivaňáková, "Changes in climate and changing climate regions in Slovakia", Morav. Geogr. Rep. 23, 71–82 (2015). https://doi.org/10.1515/mgr-2015-0019
17. U. P. Singh and A. K. Mittal, "Testing reliability of the spatial Hurst exponent method for detecting a change point", J. Water Clim. Change 12, 8, 3661–3674 (2021). https://doi.org/10.2166/wcc.2021.097
18. P. Miklánek, M. Martincová, P. Pekárová and I. Mészároš, "Seasonal changes of the soil temperature in different depths," in Hydrology and Water Resources, Soil, Forest Ecosystems, Marine and Ocean Ecosystems, The 13th International Multidisciplinary Scientific GeoConference SGEM 2013 (SGEM, Sofia, Bulgaria, 2013), pp. 285-292. ISBN 978-619-7105-02-5. ISSN 1314-2704.

19. T. Vihma, "Atmosphere-Snow/Ice Interactions," in Encyclopedia of Snow, Ice and Glaciers. Encyclopedia of Earth Sciences Series, edited by V. P. Singh, P. Singh and U. K. Haritashya (Springer, Dordrecht, Netherlands, 2011), pp. 66–75. Online ISBN 978-90-481-2642-2. https://doi.org/10.1007/978-90-481-2642-2

20. E. Reschenhofer, "The Bimodality Principle", Journal of Statistics Education 9, 1, 1–15 (2001). https://doi.org/10.1080/10691898.2001.11910644

21. M. Krock, J. Bessac, M. L. Stein and A. H. Monahan, "Nonstationary seasonal model for daily mean temperature distribution bridging bulk and tails", Weather and Climate Extremes 36, 100438 (2022). https://doi.org/10.1016/j.wace.2022.100438

22. R. Brázdil, M. Budíkova, I. Auer, R. Bohm, T. Cegnar, P. Faško, M. Lapin, M. Gajič-Čapka, K. Zaninovič, E. Koleva, T. Niedzwiedz, Z. Ustrnul, S. Szalai and R. O. Weber, "Trends of maximum and minimum daily temperatures in Central and Southeastern Europe", International Journal of Climatology 16, 7, 765–782 (1996). https://doi.org/10.1002/(SICI)1097-0088(199607)16:7<765::AID-JOC46>3.0.CO;2-O